CBPF-NF-069/01

Separations inside a cube

A.F.F. Teixeira*

Centro Brasileiro de Pesquisas Físicas

22290-180 Rio de Janeiro-RJ, Brazil

December, 2001

Abstract

Two points are randomly selected inside a three-dimensional euclidian cube. The value l of their separation lies somewhere between zero and the length of a diagonal of the cube. The probability density $\mathcal{P}(l)$ of the separation is constructed analytically. Also a Monte Carlo computer simulation is performed, showing good agreement with the formulas obtained.

*teixeira@cbpf.br

1 Introduction

An important problem in geometry and statistics is: given a convex compact space endowed with a metric, and randomly choosing two points in the space, find the probability density $\mathcal{P}(l)$ that these points have a specified separation l. The study of this problem has a long history [1], and recently gained considerable impetus from researchers in cosmic crystallography [2]-[19].

In a recent paper the functions $\mathcal{P}(l)$ corresponding to $2D$ disks and rectangles were obtained [20]. The methodology introduced in that work is here extended to a $3D$ euclidian cube.

2 Preliminaries

An euclidian cube with side a is assumed, occupying the location $0 < x, y, z < a$ in a cartesian frame. Randomly choosing two points A and B in the cube, we want the probability $\mathcal{P}(l)dl$ that the separation between the points lie between l and $l + dl$. The probability density $\mathcal{P}(l)$ has to satisfy the normalization condition

$$\int_0^{\sqrt{3}a} \mathcal{P}(l)dl = 1. \tag{1}$$

The calculation can be shortened if one considers the symmetries of the cube. Really, if the points A and B have been chosen, imagine the oriented segment $A'B'$ parallel to AB, with the tip A' coinciding with the origin O. The other tip B' then lies inside a larger cube, with side $2a$. Since the probability density $\mathcal{P}(l)$ clearly does not depend on which octant of the large cube contains B', there is no loose in generality in restricting the calculation to the cases where B' is in the octant $0 < x, y, z < a$.

With this assumption, the point B' has cartesian coordinates

$$B' = (l\cos\theta\cos\phi,\ l\cos\theta\sin\phi,\ l\sin\theta),$$

where both angles θ, ϕ are bound to the interval $[0, \pi/2]$; here ϕ is the azimuthal angle, while θ is the polar angle measured from the $z = 0$ plane. The corresponding tip B in the original segment must lie inside a parallelepiped with sides (see figure 1)

$$l_x := a - l\cos\theta\cos\phi, \quad l_y := a - l\cos\theta\sin\phi, \quad l_z := a - l\sin\theta. \tag{2}$$

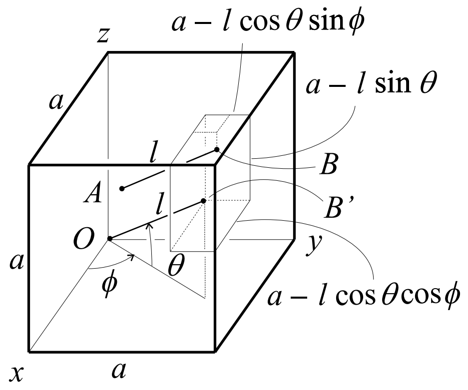

Figure 1 The endpoint B of the segment AB must lie inside the parallelepiped with a corner at $B'(l, \phi, \theta)$.

The probability $\mathcal{P}(l, \theta, \phi) dl\, d\theta\, d\phi$ that the segment AB has length between l and $l+dl$, azimuth between ϕ and $\phi + d\phi$, and polar angle between θ and $\theta + d\theta$ is then

$$\mathcal{P}(l, \theta, \phi) dl\, d\theta\, d\phi = k\, l_x\, l_y\, l_z\, l^2 \cos\theta\, dl\, d\theta\, d\phi, \tag{3}$$

where k is a constant and where the assumption $0 < \phi, \theta < \pi/2$ stands. Performing the angular integrations we shall obtain

$$\mathcal{P}(l) = \int\!\!\int \mathcal{P}(l, \theta, \phi) d\theta\ d\phi, \tag{4}$$

and we finally fix k using the condition (1).

To calculate $\mathcal{P}(l)$, three cases need be separately considered, depending on the value of l relative to a: namely the cases $0 < l < a$, $a < l < \sqrt{2}a$, and $\sqrt{2}a < l < \sqrt{3}a$.

3 The case $0 < l < a$

As is seen in the figure 2, in this case we effectively have $\phi_{min} = \theta_{min} = 0$, and $\phi_{max} = \theta_{max} = \pi/2$. Then

$$\mathcal{P}(l < a) = k\, l^2 \int_0^{\pi/2} l_z \cos\theta\, d\theta \int_0^{\pi/2} l_x\, l_y\, d\phi \tag{5}$$

$$= \frac{k\, l^2}{8}[4\pi a^3 - 6\pi a^2 l + 8 a l^2 - l^3], \tag{6}$$

where $k = 8/a^6$ as will be fixed later on.

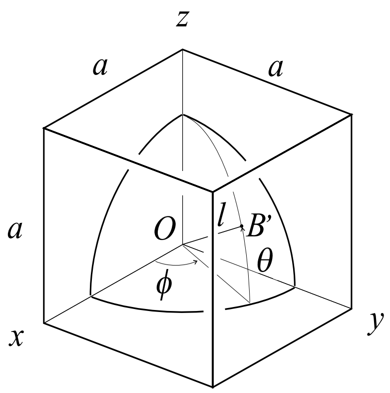

Figure 2 The triangular intersection of the $2D$ sphere with radius l and centre O with the $3D$ cube having side $a > l$.

4 The case $a < l < \sqrt{2}a$

In this case the intersection of the $2D$ sphere (with radius l) with the $3D$ cube (with side a) is an hexagonal surface as in figure 3.

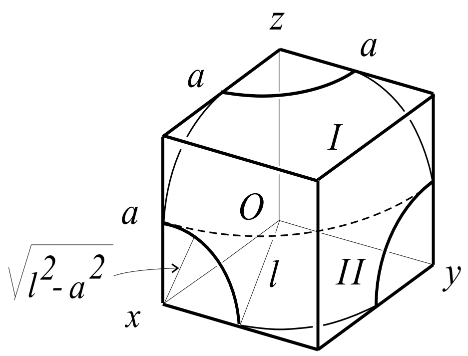

Figure 3 The hexagonal intersection of a $2D$ sphere with radius l and centre O with a $3D$ cube with a vertex in O and having side a such that $a < l < \sqrt{2}a$.

We note that the arcs of circle drawn on the faces $x, y, z = 0$ have radius l, while those drawn on the faces $x, y, z = a$ have radius $\sqrt{l^2 - a^2}$.

For convenience of integration we divide the intersection into two regions. In region I we have $\cos^{-1}(a/l) < \theta < \sin^{-1}(a/l)$ and $0 < \phi < \pi/2$.

In region II we have $\theta_{min} = 0$ and $\theta_{max} = \cos^{-1}(a/l)$. To have $\phi_{min}(\theta)$ we note that the circle drawn on the face $x = a$ satisfies the equation $\cos\phi\,\cos\theta = a/l$, so

$$\phi_{min}(\theta) = \cos^{-1}\left(\frac{a}{l\cos\theta}\right) =: \phi_1(\theta). \tag{7}$$

On the other hand, the circle drawn on the face $y = a$ satisfies $\sin\phi\,\cos\theta = a/l$, so we have

$$\phi_{max}(\theta) = \sin^{-1}\left(\frac{a}{l\cos\theta}\right) =: \phi_2(\theta). \tag{8}$$

We then find

$$\mathcal{P}(a < l < \sqrt{2}a)$$

$$= k\,l^2\left[\int_{\cos^{-1}(a/l)}^{\sin^{-1}(a/l)} \cos\theta d\theta \int_0^{\pi/2} d\phi + \int_0^{\cos^{-1}(a/l)} \cos\theta d\theta \int_{\phi_1(\theta)}^{\phi_1(\theta)} d\phi\right] l_x l_y l_z \tag{9}$$

$$= \frac{k\,l}{8}\Big[2l^4 + 6a^2l^2 - a^4 - 2\pi a^3(4l - 3a) - 8a(2l^2 + a^2)\sqrt{l^2 - a^2}$$

$$+24a^2l^2\cos^{-1}(a/l)\Big], \tag{10}$$

where $k = 8/a^6$ as will be fixed later on.

5 The case $\sqrt{2}a < l < \sqrt{3}a$

In this case the $2D$ sphere with radius l intersects the $3D$ cube with side a in the triangular surface shown in figure 4.

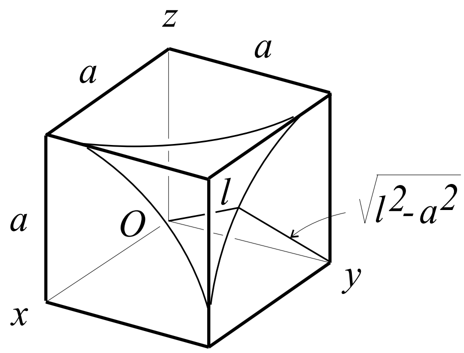

Figure 4 The triangular intersection of a $2D$ sphere with radius l and centre O with a $3D$ cube with a vertex in O and having side a such that $\sqrt{2}a < l < \sqrt{3}a$.

As before, the circles drawn on the faces $x, y, z = a$ have radius $\sqrt{l^2 - a^2}$. The azimuthal integration is performed between $\phi_1(\theta)$ and $\phi_2(\theta)$ as in the region II of the preceding case, and again $\sin\theta_{max} = a/l$; but now $\cos\theta_{min} = \sqrt{2}a/l$. We then find

$$\mathcal{P}(\sqrt{2}a < l < \sqrt{3}a) = k\,l^2 \int_{\cos^{-1}(\sqrt{2}a/l)}^{\sin^{-1}(a/l)} l_z \cos\theta d\theta \int_{\phi_1(\theta)}^{\phi_2(\theta)} l_x l_y d\phi \tag{11}$$

$$= \frac{k\,l}{8}\Big[8a(l^2+a^2)\sqrt{l^2-2a^2} - (l^2+a^2)(l^2+5a^2) + 2\pi a^2(3l^2 - 4al + 3a^2)$$
$$+24a^3 l \sec^{-1}(l^2/a^2-1) - 24a^2(l^2+a^2)\sec^{-1}\sqrt{l^2/a^2-1}\Big], \tag{12}$$

where $k = 8/a^6$.

This value for the constant k derives from the normalization condition (1), namely,

$$\int_0^a \mathcal{P}(l<a)dl + \int_a^{\sqrt{2}a} \mathcal{P}(a<l<\sqrt{2}a)dl + \int_{\sqrt{2}a}^{\sqrt{3}a} \mathcal{P}(\sqrt{2}a<l<\sqrt{3}a)dl = 1. \tag{13}$$

6 Graphs of $\mathcal{P}(l)$

In figure 5 we present a graph of the dimensionless function $a\mathcal{P}(l)$ against the dimensionless variable l/a.

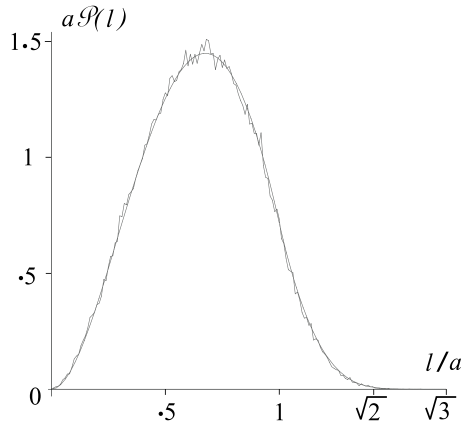

Figure 5 The probability density $\mathcal{P}(l)$ of separation l of pairs of randomly distributed points inside a cube with side a. The irregular curve is the output of a corresponding computer simulation.

We note that the function and its first derivative are continuous in the whole interval $0 < l < \sqrt{3}a$. Nevertheless the second derivative is discontinuous at $l = a$, as discussed in the next section. In the figure a normalized histogram corresponding to 150,000 separations between pairs of points randomly selected in the cube is superimposed, for comparison; the agreement of the two curves evinces the correctness of the calculation.

7 Comments

The integration to find $\mathcal{P}(l)$ in eqs. (5)-(6) is almost trivial; however, not the same can be said about the two other cases, namely in going from (9) to (10) and from (11) to (12). A computer assistance appears paramount in these two cases, to confirm every short step in the calculation and simplification of expressions.

Similarly as in [20], the probability density $\mathcal{P}(l)$ and its first derivative are continuous throughout the entire range $0 < l < \sqrt{3}a$. But the second derivative shows a finite discontinuity at $l = a$, although it is continuous at $l = \sqrt{2}a$.

A remarkable feature of $\mathcal{P}(l)$ is its behaviour for large values of l; really, near $l = \sqrt{3}a$ we find

$$a\mathcal{P}(l) = \frac{9}{5}(\sqrt{3} - l/a)^5 + O((\sqrt{3} - l/a)^6), \tag{14}$$

so $\mathcal{P}(l)$ is essentially a fifth power of $\sqrt{3} - l/a$. We find that 91% of the separations lie in the range $l \in (0, a)$, 9% lie in the interval $l \in (a, \sqrt{2}a)$, and only 0.04% have $l > \sqrt{2}a$.

References

[1] Krzysztof Bereś, *Distance distribution*, Zeszyty Naukowe Universytetu Jagiellońskiego - Acta Cosmologica - Z. 5 (1976) 7-27

[2] Kelly A. Farrar & Adrian L. Melott, *Gravity in twisted space*, Computers in Physics, Mar/Apr 1990, 185-189

[3] Roland Lehoucq, M. Lachièze-Rey & Jean-Pierre Luminet, *Cosmic crystallography*, gr-qc/9604050

[4] Helio V. Fagundes & Evelise Gausmann, *On closed Einstein-de Sitter universes*, astro-ph/9704259

[5] Roland Lehoucq, Jean-Pierre Luminet & Jean-Philippe Uzan, *Topological lens effects in universes with non-euclidian compact spatial sections*, astro-ph/9811107

[6] Germán I. Gomero, Antonio F.F. Teixeira, Marcelo J. Rebouças & Armando Bernui, *Spikes in cosmic crystallography*, gr-qc/9811038

[7] Helio V. Fagundes & Evelise Gausmann, *Cosmic crystallography in compact hyperbolic universes*, astro-ph/9811368

[8] Jean-Pierre Luminet & Boudewijn F. Roukema, *Topology of the universe: theory and observation*, astro-ph/9901364

[9] Jean-Philippe Uzan, Roland Lehoucq & Jean-Pierre Luminet, *A new crystallographic method for detecting space topology*, astro-ph/9903155

[10] Armando Bernui & Antonio F.F. Teixeira, *Cosmic crystallography: three multipurpose functions*, astro-ph/9904180

[11] Germán I. Gomero, Marcelo J. Rebouças & Antonio F.F. Teixeira, *Spikes in cosmic crystallography II: topological signature of compact flat universes*, gr-qc/9909078

[12] Germán I. Gomero, Marcelo J. Rebouças & Antonio F.F. Teixeira, *A topological signature in cosmic topology*, gr-qc/9911049

[13] Armando Bernui & Antonio F.F. Teixeira, *Cosmic crystallography: the euclidian isometries*, gr-qc/0003063

[14] Antonio F.F. Teixeira, *Cosmic crystallography in a circle*, gr-qc/0005052

[15] Roland Lehoucq, Jean-Pierre Luminet & Jean-Philippe Uzan, *Limits of crystallographic methods for detecting space topology*, astro-ph/0005515

[16] Antonio F.F. Teixeira, *Cosmic crystallography: the hyperbolic isometries*, gr-qc/0010107

[17] Germán I. Gomero, Marcelo J. Rebouças & Antonio F.F. Teixeira, *Signature for the shape of the universe*, gr-qc/0105048

[18] Evelise Gausmann, Roland Lehoucq, Jean-Pierre Luminet, Jean-Philippe Uzan & Jeffrey Weeks, *Topological lensing in spherical spaces*, gr-qc/0106033

[19] Janna Levin, *Topology and the cosmic microwave background*, gr-qc/0108043

[20] Antonio F.F. Teixeira, *Distances in plane membranes*, physics/0111108